Proceedings of the ASME 2025
International Mechanical Engineering Congress and Exposition
IMECE2025
November 16-20, 2025, Memphis, TN, USA

IMECE2025-166019

A PHOTOGRAMMETRY-BASED APPROACH FOR PATIENT-SPECIFIC MODELING IN SYNDACTYLY SURGERY: PROTOTYPING, 3D RECONSTRUCTION, AND FINITE ELEMENT ANALYSIS

Xiangyi Cheng[1], Hunter G. Geibel[2], Samuel J. Clawson[2], Yewon Jang[3], Tomas C. Hastings[2], Flint S. Guerra[2], Patrick D. Bak[2], Guang Yang[4], Vladimir T. Herdman[2], Carter M. Betts[2], Hui Shen[2]

[1]Loyola Marymount University, Los Angeles, CA
[2]Ohio Northern University, Ada, OH
[3]Hanyang University, Seoul, South Korea
[4]China-Japan Union Hospital of Jilin University, Changchun, China

ABSTRACT

Syndactyly, a congenital condition in which fingers or toes are fused, often requires surgical intervention to restore both function and aesthetics. The procedure involves separating the fused digits, reconstructing the web space, and covering the exposed areas with a dorsal flap harvested from the patient. A major challenge in this process is determining the optimal size and shape of the dorsal flap for individuals. Our research aims to provide an objective, quantitative framework for improving surgical outcomes by generating patient-specific 3D models and using finite element analysis (FEA) for dorsal flap optimization.

As a preliminary study, this work has two main objectives: 1) developing a photogrammetry system capable of 3D reconstructing accurate hand models and 2) performing FEA to analyze stress and strain distribution in the web space from the reconstructed model to refine the dorsal flap design. A prototype with four rotating arms, each holding a camera, was built to create 3D models of the hand. A real hand was scanned and reconstructed using it, and key flap parameters were extracted from the model to perform FEA evaluating a hexagonal flap design. The FEA result reveals high stress concentrations at the four corners of the flap, especially along the top edge where the flap is stretched and sutured to the palmar commissure.

This finding demonstrates the potential of integrating computational modeling into preoperative planning through FEA to improve flap design. Future work will focus on expanding the system's analytical scope, enhancing automation, exploring effective ways to present FEA results, and improving clinical integration to advance personalized surgical planning.

Keywords: photogrammetry, prototyping, syndactyly, finite element analysis, finite element modeling, optimization.

1. INTRODUCTION

Syndactyly is one of the most prevalent congenital deformities of the hand, resulting from the incomplete separation of adjacent digits during embryonic development. Surgical correction of the syndactyly condition generally required to separate the digits, reconstruct the interdigital web space, and restore adequate soft tissue coverage. A key component of the reconstructive procedure is the restoration of the web space commissure. Anatomically, the ideal commissure forms a slope of approximately 45–50^{o} from dorsal to palmar and extends halfway down the proximal phalanx [1]. To achieve this configuration, surgeons typically employ dorsal local skin flaps and/or autologous skin grafts, often harvested from the forearm. Over the years, various skin flap geometries have been introduced for web space reconstruction, including rectangular [2], hexagonal [3], pentagonal [4], omega-shaped [5], cross-shaped [6], bilobed [7] and gull wing designs [8]. Figure 1 illustrates a few flap designs in the surgery. The shape and dimensions of the flap are critical to the surgical outcome, influencing both the functional restoration and the aesthetic appearance of the reconstructed web. However, despite decades of clinical practice, no consensus has been reached on the most effective flap design. Flap selection largely depends on the surgeon's individual experience, training, and subjective judgment, which introduces variability into surgical outcomes [2]. This subjectivity may result in over- or under-utilization of skin flap tissue. Moreover, post-operative stress and strain distributions on the flap, caused by its dimension and shape, significantly influence healing outcomes, including digit mobility and the risk of web creep or tissue necrosis [9]. To address this, this study aims to introduce an objective,

quantifiable methodology into the surgical planning of syndactyly reconstruction.

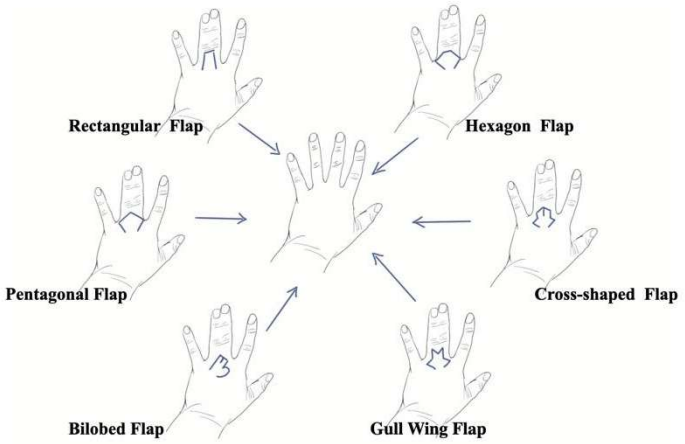

FIGURE 1: VARIOUS FLAP DESIGNS USED IN WEB SPACE RECONSTRUCTION SURGERY

Unlike engineering applications that deal with uniform and well-characterized materials and design models, human anatomy is highly variable, posing challenges to standardization in surgical procedures. However, most human bodies exhibit symmetry or near-symmetry—particularly between the left and right hands. This anatomical consistency offers an opportunity: the unaffected hand can serve as a geometric reference or "target model" for reconstructing the affected hand. Specifically, the web space geometry of the normal hand can guide the design of a patient-specific skin flap for optimal function. Therefore, the objective of this research is to prototype a photogrammetry-based system capable of capturing a high-fidelity 3D model of the unaffected hand, and to apply finite element analysis (FEA) to this model to optimize dorsal flap design. The results of FEA reveal whether the size and geometry of the flap can provide sufficient tissue coverage while maintaining appropriate stress distribution in the reconstructed web space. Therefore, the preliminary study has two primary objectives:

1) To develop a photogrammetry system capable of 3D reconstructing accurate hand models, and
2) To perform FEA to analyze stress and strain distribution in the web space from the reconstructed model to refine the dorsal flap design.

The following sections present the development of the photogrammetry system, results, numerical evaluation, followed by the discussion and conclusion.

2. SYETEM DEVELOPMENT

This section outlines the development process of the system prototype, which aims to address the first primary objective of the research. Notably, commercial 3D scanners are often expensive and may not offer the precise control over camera positioning required for capturing complex hand geometries relevant to surgical planning. The self-developed system can also provide the flexibility to incorporate future features, such as skin property measurement, automated programmable input for FEA aligned with both the primary and secondary objectives, and various methods for displaying results in clinical settings. Therefore, a photogrammetry-based prototype was developed to provide a low-cost, adjustable, and task-specific solution.

The prototype is expected to perform a full scan of the hand, capturing a sequence of images necessary for reconstructing a 3D hand model. The image acquisition process is automated to ensure consistency and accuracy. The captured images are then processed using photogrammetry software, which reconstruct a 3D mesh representation of the user's hand. The geometry of the reconstructed hand serves as a reference for evaluating the design of the dorsal skin flap in FEA.

2.1 Hardware Design

The hardware was developed to facilitate accurate 3D photogrammetric reconstruction of the human hand. Its primary mechanical feature is the ability to perform a full scan around a stationary hand by rotating four support arms, each equipped with an adjustable-position camera. Figure 2a shows the CAD assembly of the design, while Figure 2b shows the fabricated device. With four cameras, a 90° rotation ensures complete coverage from all angles. This mechanism ensures fast and comprehensive image acquisition from multiple angles, which is critical for accurate 3D reconstruction. The hand rests on an ergonomically designed palm support, featuring a contoured hand plate and adjustable base. Integrated into the frame with two aluminum bars, the palm support minimizes user fatigue.

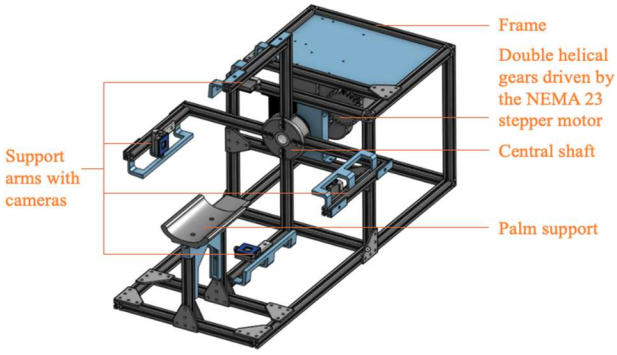

(a) CAD assembly of the design

(b) Fabricated device

FIGURE 2: DESIGN OF THE PROTOTYPE

The overall frame of the prototype is constructed using T-slotted aluminum for structural strength, modularity, and flexibility. Additionally, the prototype features a NEMA 23 stepper motor (237 oz-in torque) paired with a Pololu Tic 36v4 controller to enable precise rotational control. It drives a central shaft via double helical gears configured in a 1:1 ratio, which minimizes backlash and ensuring smooth rotation of the support arms. The central shaft, made of 1-inch polyvinyl chloride (PVC) pipe, serves a dual purpose: transmitting rotational motion and housing internal wiring to prevent tangling. The electronics, including the stepper motor controller and power supply, are housed in a dedicated mounting plate that isolates them from rotating parts. This plate is composed of two interlocking PLA sections for ease of assembly.

2.2 Vision System and Computing Device

The vision system includes four cameras integrated into the prototype (see Figure 2), which allows fast, multi-angle image capture of the hand during a 90° rotation. The use of T-slotted aluminum for camera mounting allows for adjustable camera placement. This enables different camera angles relative to the model during testing. Additionally, the setup allows for modifications to the surrounding lighting to evaluate its effects under different conditions. The cameras are implemented in Python using the OpenCV library, an open-source computer vision and machine learning software library. The prototype rotates incrementally, with OpenCV capturing images at each predefined step. Each image is saved in JPEG format within a directory named for the current test. Additionally, the captured images are resized to 200×150 pixels for live display in the user interface's preview zone, which is discussed in Section 2.3.

The system is operated using a Dell Precision 7680 computer, equipped with an Intel 20 Core i7 processor, 32 GB of RAM, and a 500 GB SSD. Note that the computer handles both the vision system and motor control.

2.3 Graphical User Interface

To facilitate user interaction and simplify the process of executing tests, a custom graphical user interface (GUI) was developed using Tkinter and OpenCV libraries. Figure 3 presents the GUI developed for the system. The left side of the interface contains a panel with a text input field for labeling the directory where test images will be stored, along with three buttons named Run Program, Preview, and Quit Program. The right side features a live preview area that displays the camera feeds in real time before testing begins. Upon launching the GUI, camera connections are initiated through OpenCV. Clicking the "Run Program" button triggers a command to begin rotating the support arms. At each predefined step, the cameras capture an image, which is then stored in a directory named based on the input in the naming field. This process repeats to collect a total of 48 images, with 12 captured by each of the four cameras. After image capture is complete, the arms return to their starting position without taking additional photos. The "Preview" button enables the viewing of the hand before initiating the photography sequence to ensure proper hand placement and framing. Clicking the "Quit Program" initiates a cleanup routine to release any remaining resources and safely terminate the program.

2.4 Reconstruction with Photogrammetry

Photogrammetry is the process of extracting information from photographs to generate 3D models of objects. A high-fidelity model allows for accurate extraction of key points from the model, thereby producing reliable FEA results for the dorsal flap. As a preliminary study, this study uses 3DF Zephyr Free, a free version of the commercial photogrammetry software developed by 3Dflow.

Before feeding the images into 3DF Zephyr Free, all 48 images captured by the four cameras are automatically processed to remove their backgrounds using Python. This step enhances the quality of the resulting 3D model, as background elements can sometimes interfere with the alignment algorithm of the reconstruction. The images are then imported into the software in a specific order to ensure proper alignment. Once the reconstruction is complete, the model is exported as an OBJ file for key point extraction and subsequent FEA. The FEA aims to analyze the stress and strain distribution on the flap applied to the reconstructed web space to refine the dorsal flap design. Figure 4 illustrates the framework of the proposed approach, designed to improve outcomes in syndactyly reconstruction surgery. Note that the dashed lines indicate future work that is beyond the scope of this current study.

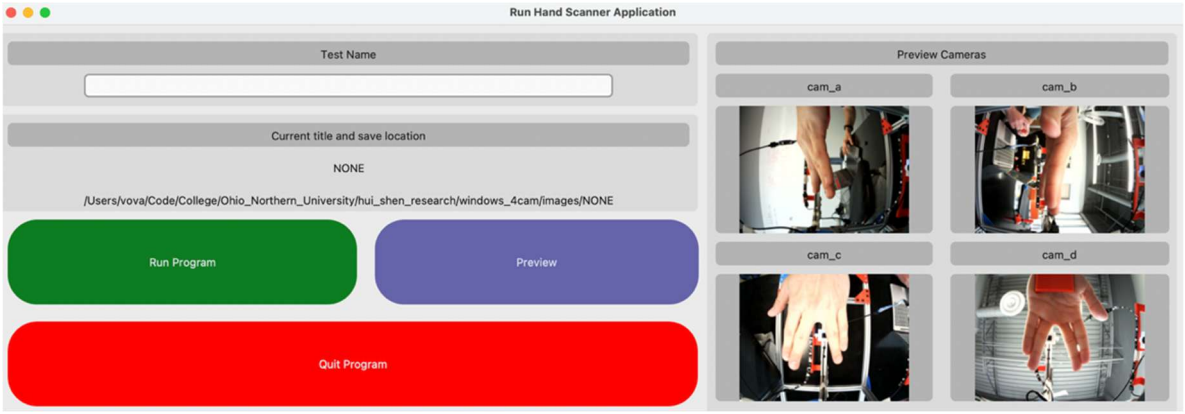

FIGURE 3: GUI DEVELOPED FOR THE SYSTEM

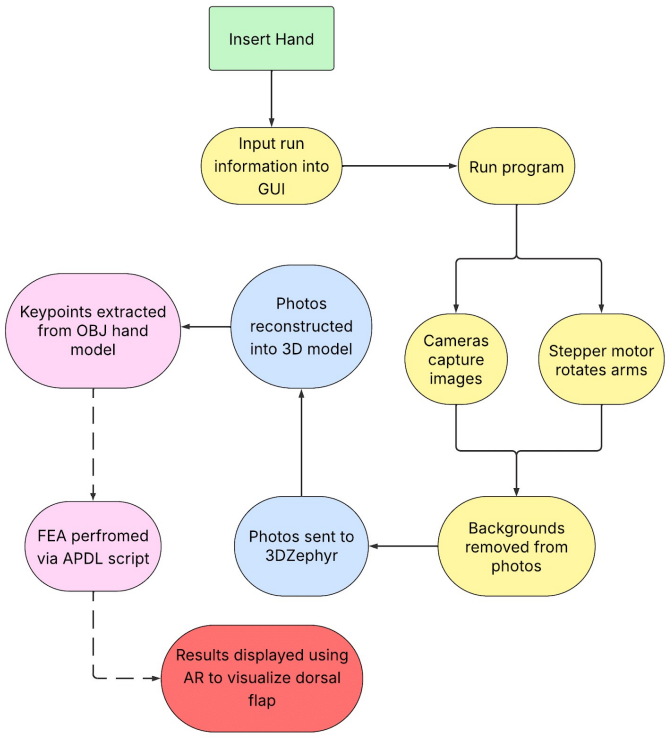

FIGURE 4: FRAMEWORK OF THE PROPOSED APPROACH DESIGNED TO IMPROVE OUTCOMES IN SYNDACTYLY RECONSTRUCTION SURGERY (SOLID LINES REPRESENT COMPLETED WORK; DASHED LINES INDICATE FUTURE WORK)

3. NUMERICAL EVALUATION

Besides developing the photogrammetry system, another objective of this study is to use the key geometry-derived parameters from the reconstructed hand model to perform FEA. This aims to evaluate stress and strain distribution on the flap placed within the reconstructed web space, with the goal of optimizing the dorsal flap design. For example, excessively high stress and strain levels can lead to tissue damage, impaired healing, and increased risk of complications. If such stress concentrations are observed, surgeons may consider increasing the flap size or altering the flap shape to achieve better surgical performance. As a preliminary study, the FEA presented in this section serves as a proof-of-concept for the application of the system. Therefore, instead of performing FEA automatically using an ANSYS Parametric Design Language (APDL) script as proposed in Figure 4, we manually imported the reconstructed hand model into ANSYS. Additionally, only one flap design, the hexagonal skin flap, was selected to evaluate the feasibility of the approach. Originally proposed in [3], the hexagonal flap is one of the commonly used designs in syndactyly reconstruction surgery. Figure 5a shows the cut lines adopted to harvest the hexagonal flap from the hand, and Figure 5b illustrates the sutured web space after surgery using the hexagonal flap. The dimensions of the hexagonal skip flap depend on anatomical data from the patient's hand, including distances between key landmarks such as knuckles, joints, and finger radii [3]. Due to the symmetry or near-symmetry between the left and right hands, these dimensions can be obtained by scanning the unaffected hand prior to surgery and then applied to the affected hand during the procedure. Specifically, the flap height is defined as two-thirds of h, as shown in Figure 6, where h is the distance from the knuckle (metacarpophalangeal joint) to the first joint (proximal interphalangeal joint) of the middle finger. The flap width w is calculated using Equation (1), where r is the radius of the web space. The top and bottom edges of the hexagon are each one-third of w. The hexagonal shape is symmetrical along both the horizontal and vertical axes.

$$w = \pi r + 2r \tag{1}$$

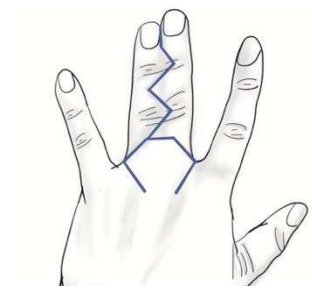

(a) Cut lines adopted to harvest the hexagonal flap

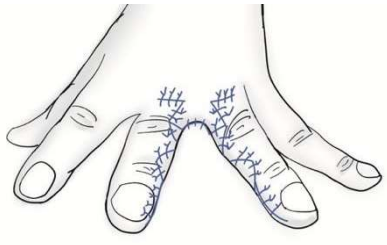

(b) Sutured web space after surgery using the hexagonal flap

FIGURE 5: THE DORSAL HEXAGON FLAP PROPOSDED IN [3]

To ensure patient specificity, the size of the evaluated hexagonal flap (i.e., the parameters h and w) was determined from a hand model reconstructed by the prototype based on a real hand without syndactyly. This hand was treated as the unaffected hand of a patient with syndactyly. Figure 6 presents the skin flap, with dimensions defined from the model scanned using the prototype, where $w = 57.5mm$ and $h = 31.8mm$. The region below the skin flap represents the skin on the back of the hand to which the flap is connected.

After the skin flap design was obtained based on anatomical data from the scanned hand, the suturing procedure for attaching the flap to the web space commissure between the middle and ring fingers was expected to be simulated through FEA, as

shown in Figure 7. Note that the surface of the web space commissure is a complex 3D surface which must be reconstructed during surgery. Its complex geometry presents challenges for modeling flat skin flap coverage and suturing using FEA due to the numerical difficulty of solving 3D contact problems. To address this, the 3D surface of the web space commissure from the scanned model was unrolled into a 2D plane using a built-in function in ANSYS software. This method, proposed in [10], facilitates the application of boundary and loading conditions when analyzing stress and strain in stretched skin flaps. The resulting 2D unrolled surface was then used to determine the boundaries and loading conditions. In the FEA model (see Figure 6), the two vertical sides and the bottom edges of the rectangular back skin section were fixed. As the flap width w closely matched the maximum width of the unrolled web space commissure in this case, zero displacement was applied along the x-direction. To simulate stretching across the web space commissure toward the distal end on the palmar side, a displacement of $12.7mm$ (that is the difference between two-thirds of h and the unrolled web space commissure from the scanned model) was applied along the y-direction at the top edge of the skin flap.

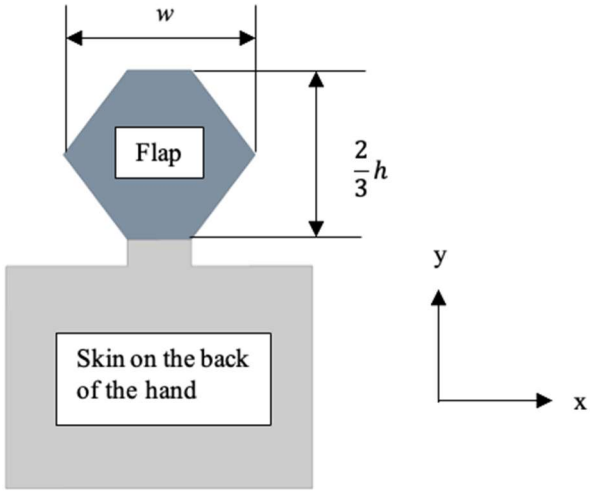

FIGURE 6: FINITE ELEMENT MODEL OF THE FLAP AND THE SKIN ON THE BACK OF THE HAND

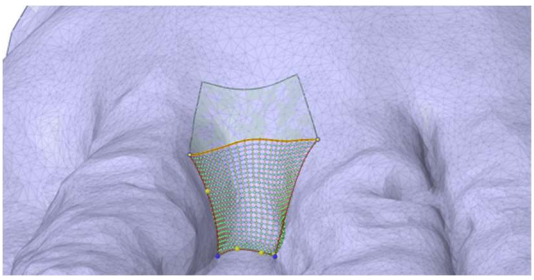

FIGURE 7: SCANNED MODEL OF THE UNAFFECTED HAND IMPORTED INTO ANSYS, WITH THE HIGHLIGHTED REGION REPRESENTING THE WEB SPACE COMMISSURE TARGETED FOR RECONSTRUCTION

The material properties of the skin were defined with a Young's modulus of 0.12 MPa and a Poisson's ratio of 0.49 [11]. After the skin flap was stretched to the final desired shape, the von Mises stress distribution was obtained from ANSYS, as shown in Figure 8. The result shows high stress concentrations near the four vertices at the bottom and top, particularly along the top edge where the flap is stretched and stitched to the palmar edge of the web space commissure. This stress distribution result is consistent with the observed post-surgical tissue necrosis and sloughing at the palmar end of the web space, as reported in clinical findings [4].

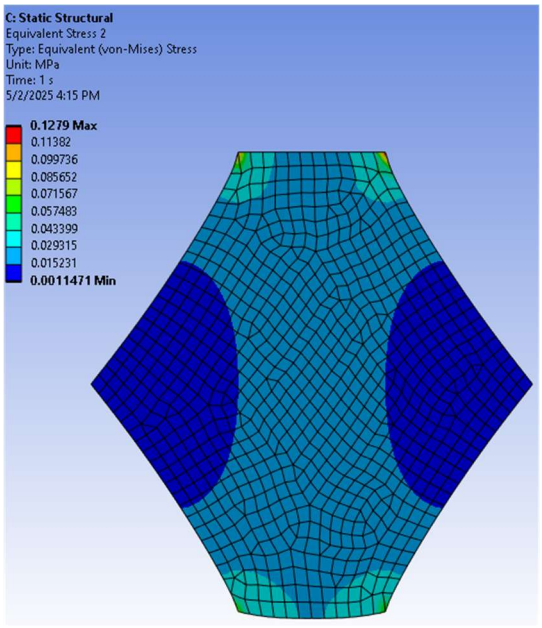

FIGURE 8: VON MISES STRESS DISTRIBUTION ON THE HEXAGONAL FLAP OBTAINED FROM FEA

4. DISCUSSION

The consistency between our FEA results and clinical observations demonstrates that our approach, including both prototyping and FEA, can serve as a foundation for optimizing flap design, as an optimal design should exhibit relatively uniform stress and strain following surgery. High stress concentrations should be avoided as they may lead to tissue necrosis [9]. Additional clinical data, including patient-specific anatomical measurements and postoperative outcomes, would enhance the accuracy of the model and support its validation by allowing comparison between simulated and actual surgical results.

Despite the promising results, there are limitations in both the prototype and the conducted FEA. For the prototype, one limitation is the inconsistent lighting conditions, often caused by external environmental factors, which can negatively impact image quality and reduce the accuracy of 3D reconstruction. Another significant challenge lies in the palm identification process within 3D Zephyr Free, which occasionally fails to reliably distinguish anatomical features, leading to errors in

model generation and subsequent analysis. To address these issues, we plan to add a lighting source to the prototype to ensure consistent illumination and to develop custom algorithms for more robust 3D hand reconstruction.

A key limitation of skin flap FEA is that stress distribution is influenced not only by the flap's shape and size but also by the mechanical properties of the skin, such as Young's modulus. For patients with a lower Young's modulus, which indicates more elastic skin, the same flap design would result in lower stress. This implies that, to achieve the same post-surgical stress level, a more elastic skin can accommodate a smaller flap. Since younger patients tend to have more elastic skin (i.e., a lower Young's modulus) [11], smaller flaps may be sufficient for surgeries performed at a younger age. Ideally, optimal flap design should be personalized based on individual hand anatomy and skin properties. However, the mechanical properties of human skin vary widely due to individual differences such as age, gender, and anatomical location, as well as the experimental methods used to measure them. Yazdi et al. reviewed over 130 studies and highlighted the inconsistencies, with reported Young's modulus values ranging from as low as 1.09 kPa to over 80 MPa [12]. This presents significant challenges for accurately modeling skin behavior in patient-specific FEA for flap design. Future studies should aim to improve non-invasive methods for determining patient-specific mechanical properties prior to surgery. These parameters can then be used as inputs for FEA, as noted and recommended in [13, 14].

Future work will also focus on expanding the system's analytical scope, enhancing automation, and improving clinical integration to advance personalized surgical planning. We only evaluated one flap shape in this study due to the scope of this preliminary study, so a key direction involves evaluating a broader range of skin flap designs. By systematically analyzing the biomechanical performance of various flap shapes and sizes, the system can reveal how different shapes and sizes affect stress distribution and tissue coverage. This comparative analysis will help identify design trends and support evidence-based decision-making tailored to patient-specific anatomy. The long-term goal is to enable more personalized and optimized surgical planning in reconstructive procedures. Further enhancements will focus on automating the FEA process through the integration of APDL, shown in Figure 6. This will enable direct import of geometric parameters from the photogrammetry system and support iterative adjustment of flap configurations. Stress and strain distributions will be recalculated after each iteration, with the goal of converging on optimal designs. Animated simulations of these iterations will offer both quantitative insights and intuitive visual feedback, serving as a powerful tool for preoperative planning. To make these tools more accessible in clinical environments, future work will also explore the integration of mixed reality and augmented reality technologies (see Figure 6). These immersive interfaces will allow surgeons to interact with 3D models and simulation results in an intuitive way, which bridges the gap between engineering analysis and surgical practice.

5. CONCLUSION

This study presents a framework to quantify and optimize the surgical process for syndactyly by 1) developing a photogrammetry system capable of 3D reconstructing accurate hand models and 2) performing FEA to analyze stress and strain distribution in the web space from the reconstructed model to refine the dorsal flap design. A prototype system was developed to perform accurate 3D photogrammetric reconstruction of the human hand using four cameras mounted on motorized rotating arms. Image capture is automated through a custom GUI, which streamlines the acquisition process. The captured images undergo background removal to enhance model quality and are subsequently processed in 3DF Zephyr Free for 3D reconstruction. We scanned a real hand without syndactyly using the prototype and treated as an unaffected hand of a patient with syndactyly. To evaluate the feasibility of using FEA for dorsal flap design optimization, the commonly used hexagonal skin flap was analyzed, with its size determined from the scanned model. The FEA result shows elevated stress near the four corners of the flap, particularly along the top edge where it is stretched and sutured to the palmar side of the web space commissure. This pattern is consistent with surgical observations. This suggests that FEA holds great potential as a tool for guiding the refinement of flap design.

ACKNOWLEDGEMENTS

The authors gratefully acknowledge the 2024 Summer Research Grant provided by the College of Engineering at Ohio Northern University.

REFERENCES

[1] Kozin SH. Syndactyly. Journal of the American Society for Surgery of the Hand. 2001 Feb 1;1(1):1-3.

[2] Braun TL, Trost JG, Pederson WC. Syndactyly release. InSeminars in Plastic Surgery 2016 Nov (Vol. 30, No. 04, pp. 162-170). Thieme Medical Publishers.

[3] Wang S, Zheng S, Li N, Feng Z, Liu Q. Dorsal hexagon local flap without skin graft for web reconstruction of congenital syndactyly. The Journal of Hand Surgery. 2020 Jan 1;45(1):63-e1.

[4] Gao W, Yan H, Zhang F, Jiang L, Wang A, Yang J, Zhou F. Dorsal pentagonal local flap: a new technique of web reconstruction for syndactyly without skin graft. Aesthetic plastic surgery. 2011 Aug;35:530-7.

[5] D'arcangelo M, Gilbert A, Pirrello R. Correction of syndactyly using a dorsal omega flap and two lateral and volar flaps: a long-term review. Journal of Hand Surgery. 1996 Jun;21(3):320-4.

[6] Yu W, Yang G, Yin F, Yin C, Yang W, Chan PT, Shen X. A new concept of webspace reconstruction in syndactyly-An easily reproducible cross-shaped advancement flap. Journal of Hand and Microsurgery. 2024 Oct 1;16(4):100081.

[7] Sahin C, Ergun O, Kulahci Y, Sever C, Karagoz H, Ulkur E. Bilobe flap for web reconstruction in adult syndactyly release: a new technique which can avoid the use of skin graft. Plastic and Reconstructive Surgery. 2015 Oct 1;136(4S):28-9.

[8] Tian X, Xiao J, Li T, Chen W, Lin Q, Chim H. Single-stage separation of 3-and 4-finger incomplete simple syndactyly with contiguous gull wing flaps: a technique to minimize or avoid skin grafting. The Journal of Hand Surgery. 2017 Apr 1;42(4):257-64.

[9] Ogawa R, Okai K, Tokumura F, Mori K, Ohmori Y, Huang C, Hyakusoku H, Akaishi S. The relationship between skin stretching/contraction and pathologic scarring: the important role of mechanical forces in keloid generation. Wound Repair and Regeneration. 2012 Mar;20(2):149-57.

[10] Ji X, Wen G, Gong H, Sun R, Li H. Three-dimensional wound flattening method for mapping skin mechanical properties based on finite element method. Computer Methods in Biomechanics and Biomedical Engineering. 2024 Jan 25;27(2):237-50.

[11] Chen L, Yang X, Zhang Y, Zhang L, Xia Y. Evaluation and comparison of reading man flap based on different designs of angles and central axial lengths using finite element method. Scientific Reports. 2025 Jan 22;15(1):2803.

[12] Yazdi SJ, Baqersad J. Mechanical modeling and characterization of human skin: A review. Journal of biomechanics. 2022 Jan 1;130:110864.

[13] Myoung J, Jeong ET, Kim M, Lim JM, Kang NG, Park SG. Validation of the elastic angle for quantitative and visible evaluation of skin elasticity in vivo. Skin Research and Technology. 2021 Nov;27(6):1017-22.

[14] Yang G, Shen H, Jang Y, and Cheng X, Finite Element Analysis-Assisted Surgical Planning and Evaluation of Flap Design in Hand Surgery, Frontiers in Bioengineering and Biotechnology, under review.